Scattering of ultracold atoms by absorbing nanospheres

Florian Arnecke, Harald Friedrich, and Javier Madroñero
Physik Department, Technische Universität München, 85747 Garching
(Received 19 December 2006; published 25 April 2007)

We study elastic scattering of ultracold atoms by a conducting sphere. Loss of flux through inelastic reactions and adsorption is described in an unambiguous and model-independent way by incoming boundary conditions in the semiclassical region near the surface of the sphere. Differential cross sections are presented for Na and metastable He($2\,^3S$) atoms scattered by a nanosphere with radius 200 a.u. or 2000 a.u. Their near-threshold behavior is determined by a small number of parameters which are properties of the potential tail beyond the semiclassical regime, and it depends sensitively on the characterstic lengths β_6, β_7 which describe the strength of the nonretarded van der Waals part and the highly retarded Casimir part of the atom-sphere interaction, respectively. These lengths can be tuned to probe various regions of the atom-sphere interaction by appropriate choice of the radius of the sphere.

DOI: 10.1103/PhysRevA.75.042903 PACS number(s): 34.50.Dy, 03.65.Nk, 03.75.−b

I. INTRODUCTION

Understanding the interaction of ultracold atoms with surfaces is a prerequisite for the design and construction of atomic waveguides and other atom-optical devices [1]. When an atom comes close to a conducting or dielectric surface, within a dozen atomic units or less, the atom-surface interaction is generally quite complex and leads to inelastic reactions and adsorption ("sticking"). Beyond this close region, the interaction can be described by a local potential $V(s)$ depending on the distance s of the atom from the surface. When the surface is flat, the potential behaves as a van der Waals potential, $V(s)=-C_3/s^3$, for "small" distances $s\to 0$, which are however still beyond the close region where inelastic reactions and sticking occur. For large distances, retardation effects become important, and the potential behaves as $V(s)=-C_4/s^4$ as first described by Casimir and Polder in 1948 [2]. The coefficients C_3 and C_4 depend on the polarizability properties of the atom and on the dielectric properties of the (flat) surface. For a conducting surface and an atom in a spherical state $|\psi_0\rangle$,

$$C_3=\frac{\langle\psi_0|\vec{d}^2|\psi_0\rangle}{12}=\frac{1}{4\pi}\int_0^\infty \alpha_d(i\omega)d\omega,\quad C_4=\frac{3}{8\pi}\frac{\alpha_d(0)}{\alpha_{fs}}, \tag{1}$$

where α_d is the dipole polarizability of the atom and α_{fs} is the fine-structure constant [3,4]. In the "transition zone" between the nonretarded van der Waals regime of small distances and the highly retarded regime of large s, the potential undergoes a smooth transition from the $-C_3/s^3$ behavior to the $-C_4/s^4$ behavior. The ratio

$$\frac{C_4}{C_3}=L \tag{2}$$

is a typical length scale for this zone. If we visualize the polarizability of the atom as essentially due to one "mean" dipole transition matrix element $\langle\psi_0|\vec{d}|\psi_1\rangle$, then $2\pi L$ approximately corresponds to the wavelength λ_{01} of this mean transition. (Note, however, that the model of a two-level atom in general does not satisfy oscillator strength sum rules and is not very suitable for calculating atom-surface potentials [3].)

At sufficiently low energies, atom-surface collisions are strongly influenced by quantum effects, such as quantum reflection [5] by the nonclassical region in coordinate space, sometimes called "badlands" [6,7], which is typically located at distances of many hundreds or thousands of atomic units in the purely attractive tail of the atom-surface potential. Since the probability for quantum reflection tends to unity at threshold, this effect is always important at sufficiently low energy, and it has recently been studied intensely, both experimentally [8–14] and theoretically [7,15–20]. For most realistic examples of an atom in front of a flat surface, quantum reflection probabilities are essentially determined by the asymptotic, highly retarded Casimir part of the atom-surface potential, $-C_4/s^4$, and they are largely insensitive both to the nonretarded van der Waals part of the potential at smaller distances and to the shape of the potential in the transition zone [7].

More flexible probing of atom-surface interactions can be achieved in the scattering of atoms by a sphere. Observable cross sections depend strongly not only on the modulus but also on the phase of the scattering matrix. Moreover, the radius of the sphere may be regarded as a tunable parameter that can be adjusted to probe different regimes of the atom-sphere potential. In this paper we describe the elastic scattering of polarizable atoms by a conducting sphere with a radius in the nanometer range. In Sec. II we discuss the general structure of the atom-sphere potential and in Sec. III we describe the leading near-threshold contributions to the differential cross section. Concrete examples involving sodium and metastable helium atoms are given in Sec. IV.

II. ATOM-SPHERE POTENTIAL

When the distance s of the atom from the surface of the sphere is small compared to the radius R of the sphere—but still beyond the "close" region of inelastic reactions and adsorption—the potential can be expected to be as for an

atom in front of a flat surface. Such an atom-surface potential can be written as

$$V_{\text{flat}}(s) = -\frac{C_3}{s^3 v(s/L)}, \tag{3}$$

with L given by (2). The coefficients C_3 and C_4 are as defined in (1), and $v(x)$ is a factor defining the shape of the potential in the transition zone. Its asymptotic properties are defined by

$$v(x) \sim \begin{cases} 1, & x \to 0, \\ x, & x \to \infty. \end{cases} \tag{4}$$

When the distance s of the atom from the surface of the sphere is large compared to the radius R of the sphere, the atom-sphere potential behaves as a nonretarded van der Waals potential, $V(s)=-C_6/s^6$, for "small" distances (still larger than R) and as a highly retarded Casimir potential, $V(s)=-C_7/s^7$, for large distances. Such a potential may be written as

$$V_{\text{sphere}}(s) = -\frac{C_6}{s^6 v(s/L')}, \tag{5}$$

where

$$L' = \frac{C_7}{C_6} \tag{6}$$

and v is again a shape factor obeying the boundary conditions (4). The coefficients C_6 and C_7 depend on the polarizability properties of both the atom and the sphere. For a conducting sphere with a frequency-independent dipole polarizability equal to R^3, they are related to the corresponding strengths C_3 [21] and C_4 [22] in (1) by

$$C_6 = 12R^3 C_3, \quad C_7 = \tfrac{46}{3} R^3 C_4. \tag{7}$$

The length L' as defined in (6) is independent of R and close in value to the length L defined in (2) for the case of a flat surface,

$$L' = \tfrac{23}{18} L. \tag{8}$$

Both L and L' are typical lengths in the transition zone between the nonretarded van der Waals part of the potential at small distances and the highly retarded part at large distances.

An atom-surface potential obeying the correct boundary conditions in all cases, i.e., depending on whether the distance s is small or large compared to the radius of the sphere and whether it is small or large compared to distances characteristic of the transition zone, can be constructed by combining (3) and (5),

$$V(s) = -\left[\frac{s^3}{C_3} v\left(\frac{s}{L}\right) + \frac{s^6}{C_6} v\left(\frac{s}{L'}\right)\right]^{-1}, \tag{9}$$

and we use one shape factor v for both terms in the square bracket for simplicity. In order to appreciate the importance of the various contributions to the atom-surface potential, it is helpful to express the strength parameters C_α in terms of lengths β_α,

$$C_\alpha = \frac{\hbar^2}{2M} (\beta_\alpha)^{\alpha-2}, \quad \beta_\alpha = \left(\frac{2M}{\hbar^2} C_\alpha\right)^{1/(\alpha-2)}. \tag{10}$$

In these terms, we can rewrite Eq. (9) as

$$V(s) = -\frac{\hbar^2}{2M}\left[\frac{s^3}{\beta_3} v\left(\frac{s}{L}\right) + \frac{s^6}{(\beta_6)^4} v\left(\frac{s}{L'}\right)\right]^{-1}, \tag{11}$$

and L, L' are given by

$$L = \frac{(\beta_4)^2}{\beta_3}, \quad L' = \frac{(\beta_7)^5}{(\beta_6)^4}. \tag{12}$$

For the explicit applications in Sec. IV we chose two different versions of the potential (9) and (11) based on two shape factors,

$$v_1(x) = 1 + x, \quad v_2(x) = \frac{\pi/2}{\arctan[\pi/(2x)]}. \tag{13}$$

The shape factor v_1 was used by Shimizu [8] to analyze the probabilities he measured for metastable neon atoms being quantum reflected from a flat silicon surface, and the shape factor v_2 has been used by Holstein [23] to describe the transition from the nonretarded to the highly retarded regime. In the analysis of quantum reflection by flat surfaces in [7], the shape factor v_1 appeared to describe a somewhat more abrupt transition from the nonretarded regime to the highly retarded regime than was seen in a more realistic atom-surface potential, while the shape factor v_2 described a somewhat smoother transition. It seems reasonable to assume, that the behavior of a realistic atom-surface potential lies in between that described by these two shape factors.

III. ELASTIC SCATTERING

The elastic scattering amplitude $f(\theta)$ can be expanded in partial waves,

$$f(\theta) = \sum_{l \geq 0} f_l P_l(\cos\theta), \quad f_l = \frac{2l+1}{2ik}(e^{2i\delta_l} - 1), \tag{14}$$

and the scattering phase shifts δ_l are determined by solving the radial Schrödinger equation with the effective potential

$$V_{\text{eff}}(r) = V(s) + \frac{\hbar^2}{2M}\frac{l(l+1)}{r^2}, \quad r = s + R > R, \tag{15}$$

for a radial wave function obeying the asymptotic boundary condition $u_l(r) \sim \sin(kr + \delta_l - l\pi/2), (r \to \infty)$ [24]. Close to the surface of the sphere, $r \to R$, the attractive singular part $V(s)$ dominates in (15), motion becomes semiclassical, and we can describe total absorption at the surface of the sphere by imposing incoming WKB wave functions as the boundary condition in this limit. Because of the loss of flux, the S-matrix $e^{2i\delta_l}$ is no longer unitary and the scattering phase shifts δ_l are complex. In contrast to the widespread use of complex potentials to describe absorption [25], the implementation of incoming WKB boundary conditions in the semiclassical region near the surface of the sphere provides an unambiguous and model-independent treatment of the

TABLE I. Tail parameters $\mathcal{A}_0 - R = \bar{a} - ib$ and Λ and p-wave scattering length $\mathcal{A}_1(R \to 0)$ for homogeneous atom-surface potentials $V(s) = -C_\alpha / s^\alpha$ with $\alpha = 6$ or 7 in terms of the associated characteristic length β_α defined by (10).

α	$\bar{a}/\beta_\alpha$	b/β_α	$\Lambda/(\bar{a}-ib)$	$\mathcal{A}_1(R\to 0)/(\bar{a}-ib)$
6	0.4779888	0.4779888	1	−1.1687348
7	0.5388722	0.3915136	0.6496249	−1.0678594

loss of flux through inelastic reactions and sticking.

For $l=0$, there is no centrifugal potential and the radial equation is formally similar to the one-dimensional Schrödinger equation describing quantum reflection by an attractive potential diverging to large negative values at $r \to R$. The quantum reflection amplitude can be written as $-e^{2i\delta_0}$, and for small energies $E = \hbar^2 k^2/(2M)$, the leading near-threshold behavior of the complex phase shift δ_0 is

$$\delta_0 \sim -(\bar{a}_R - ib)k + \tfrac{1}{3}(k\Lambda)^3, \quad k \to 0. \tag{16}$$

Here $\bar{a}_R - ib = \mathcal{A}_0$ is the complex s-wave scattering length. The "threshold length" b determines the leading, linear decline of the quantum reflection probability from unity for the potential $V(s)$. Because the radial Schrödinger equation is defined in terms of $r = s + R$, the mean scattering length $\bar{a}_R$ is the sum of the mean scattering length $\bar{a}$ of the potential $V(s)$ and the radius R of the sphere,

$$\mathcal{A}_0(R) = \bar{a} + R - ib. \tag{17}$$

Both $\bar{a}$ and b are "tail parameters" of the potential $V(s)$, which can be derived from the threshold solutions of the Schrödinger equation beyond the semiclassical region at "small" distances [26]. Λ is a further tail parameter of $V(s)$ which follows from an adaptation of effective-range theory to quantum reflection [27]. For any potential $V(s)$ falling off faster than $-1/s^5$ asymptotically, $\bar{a}$, b, and Λ are well-defined finite numbers which are characteristic of the potential tail beyond the semiclassical region at small distances. For a homogeneous potential, $-C_\alpha/s^\alpha$, they are related to the length paramater β_α given by (10) via coefficients depending in a simple analytic way on the power α, see [27] and Table I. The tail parameters $\bar{a}$, b, and Λ do not depend explicitly on the radius R of the sphere, but they do depend implicitly on R, because the atom-sphere potential $V(s)$, e.g., as defined in (9) and (11), depends on R through the R dependence of the strength parameters C_6, C_7 or β_6, β_7.

For $l=1$, the leading contribution to the near-threshold behavior of the (complex) scattering phase shift is determined (for potentials falling off faster than $1/s^5$) by the complex p-wave scattering length $\mathcal{A}_1$,

$$\delta_1 \sim \tfrac{1}{3}[k\mathcal{A}_1(R)]^3, \quad k \to 0. \tag{18}$$

$\mathcal{A}_1$ is related to the threshold behavior of the amplitude for tunneling through the potential barrier formed by the centrifugal potential and the singular attractive potential $V(s)$, and it depends in a nontrivial way on the radius R of the sphere. Analytical expressions have been derived for the special case that $V(s)$ homogeneous and $R \to 0$, see [28,29]. Note that $\mathcal{A}_1$ is a real multiple of $\bar{a} - ib$ in this special case, see Table I.

Up to and including order $O(E)$, the differential cross section is given by the s-wave contribution and the interference term between s and p waves,

$$\frac{d\sigma}{d\Omega} = |f(\theta)|^2 \tag{19}$$

$$\sim |\mathcal{A}_0|^2(1 - 2bk) + k^2[F(l=0) + \tilde{F}(l=0,1)\cos\theta], \quad k \to 0. \tag{20}$$

Here F is a well-defined function of $\mathcal{A}_0$ and Λ, while $\tilde{F}$ also depends on $\mathcal{A}_1$.

IV. APPLICATION

For concrete calculations in realistic examples we chose two rather different types of atoms, *viz.* metastable He($2\,^3S$) atoms which are widely used in atom-optics experiments [30], and ground-state sodium atoms, which have recently been used in the study of quantum reflection of Bose-Einstein condensates [11,14]. Accurate calculations of the potential of metastable helium atoms in front of a flat surface have been performed by Yan and Babb [31], and the strength parameters describing the potential in the nonretarded and highly retarded limits are given as $C_3 = 1.9009$ a.u. and $C_4 = 5163$ a.u. for a conducting surface. For sodium atoms in front of a flat conducting surface, Kharchenko *et al.* [32] derived the parameters $C_3 = 1.889$ a.u. and $C_4 = 1417$ a.u. via an electric-dipole oscillator strength distribution constructed from combinations of experimental and theoretical energy levels, oscillator strengths and photoionization data, constrained by accurate values of oscillator strength sum rules. Their result for C_3 is consistent with more recent theoretical calculations by Derevianko *et al.* [33] and Johnson *et al.* [34] based on relativistic many-body perturbation theory.

The differential cross section up to order $O(E)$ is determined by s- and p-wave contributions only, according to (20), and the isotropic s-wave contribution can be filtered out by looking in the direction perpendicular to incidence, where the angle-dependent term proportional to $\cos\theta$ vanishes. Figure 1 shows the differential cross section (19) at $\theta = \frac{\pi}{2}$ for metastable He($2\,^3S$) atoms (top panel) and for ground-state Na atoms (bottom panel) elastically scattered by an absorbing sphere of 200 a.u. radius for wave numbers k up to $5/\mu$m. This corresponds to temperatures up to 1 μK for helium and 200 nK for sodium. The solid and dashed lines show the results obtained with the shape factors v_1 and v_2, respectively [see (13)], in the potential (9) and (11). They are quite close to the expectations for a homogeneous $-C_6/s^6$ potential (dotted-dashed lines) in the helium case, and to a homogeneous $-C_7/s^7$ potential (dotted lines) in the sodium case. The shape of the potential in the transition zone has essentially no influence on the slope, which determines the threshold length b, i.e., the imaginary part of the complex scattering length, and a small effect on the threshold value of

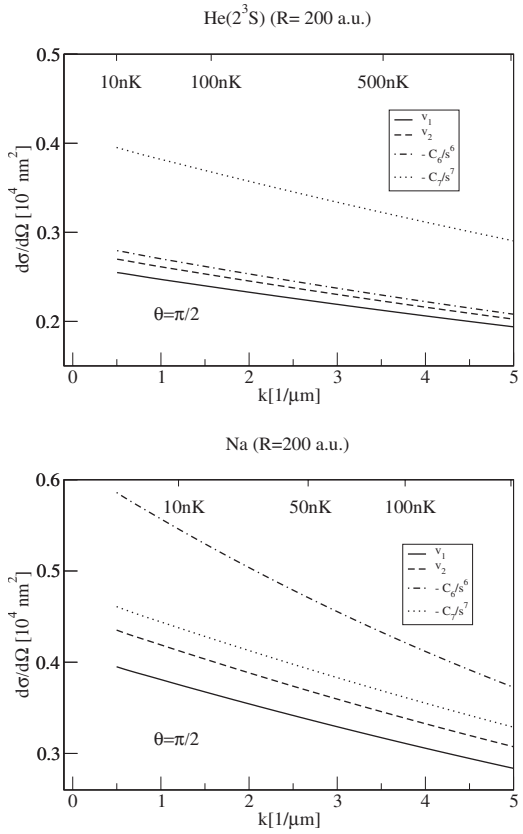

FIG. 1. Differential cross section (19) at $\theta=\frac{\pi}{2}$ for the elastic scattering of He($2\,^3S$) atoms (top panel) and ground-state sodium atoms (bottom panel) by an absorbing sphere of radius $R=200$ a.u. The parameters C_α, β_α describing the potential strength in the nonretarded van der Waals and the highly retarded Casimir limits are as given in Table II [see also (7) and (21)]. The dotted-dashed lines show the results for a homogeneous potential $-C_6/s^6$, corresponding to a nonretarded van der Waals potential, and the dotted lines show the results for a homogeneous potential $-C_7/s^7$, corresponding to a highly retarded Casimir potential. The solid and dashed lines show the cross sections obtained with the realistic atom-sphere potential (9) and (11) containing the two versions (13) for the shape factor describing the transition from the nonretarded to the highly retarded regime.

the cross section, which is simply $(\bar{a}+R)^2+b^2$ according to (20).

Although the cross sections in Fig. 1 show, at least up to order $O(E)$, only the s-wave contribution consisting of quantum reflection in the nonclassical region of the potential tail or transmission (leading to absorption) through this region, it offers more information than a corresponding measurement of quantum reflection probabilities from a flat surface, because the leading terms are sensitive to both modulus and phase of the scattering matrix. If we wanted to extract information about the potential from elastic scattering cross sections, then fitting the θ-independent part of the expression (20) to the leading near-threshold behavior of the cross section at $\theta=\frac{\pi}{2}$ would allow an easy determination of $\bar{a}$ and b, as well $F(l=0)$ which depends also on Λ. The important part of the tail of the atom-sphere potential is due to the second term in the square brackets in (9) and (11) describing the transition from $-C_6/s^6$ to $-C_7/s^7$ at distances large compared to the radius of the sphere. An effect of the flat-surface terms $-C_3/s^3$ and $-C_4/s^4$, which should be important closer to the surface, was barely noticeable in our present calculations. We checked this by dropping the contribution involving $s^3v(s/L)$ in (9) and (11), so that the potential assumed the form (5), and this only marginally affected the results. Note that knowledge of the potential strengths C_6 and C_7 determining the nonretarded and retarded limits of the potential between the atom and a conducting sphere for one given radius R implies, via (7), knowledge of C_6 and C_7 for any value of R, and of the corresponding R-independent potential strengths C_3 and C_4 determining the potential between the same atom and a flat conducting surface.

The key to understanding the different results for metastable helium and for ground-state sodium in Fig. 1 lies in an appreciation of the magnitudes of the characteristic lengths β_α associated with the potential strengths C_α according to (10). The values of β_6 and β_7 depend on the R-independent lengths β_3, β_4 and the radius R of the sphere according to (7),

$$(\beta_6)^4 = 12R^3\beta_3 \Rightarrow \beta_6 = R^{3/4}(12\beta_3)^{1/4},$$

$$(\beta_7)^5 = \tfrac{46}{3}R^3(\beta_4)^2 \Rightarrow \beta_7 = R^{3/5}\left(\sqrt{\tfrac{46}{3}}\beta_4\right)^{2/5}, \qquad (21)$$

and they are listed in Table II for $R=200$ a.u., and $R=2000$ a.u. For $R=200$ a.u., both β_6 and β_7 are noticeably smaller than the length L' in the helium case, which means that the important characteristic lengths of the potential tail lie short of the transition zone in the nonretarded van der Waals regime, so the cross sections resemble the expectations for a pure nonretarded $-C_6/s^6$ potential tail. For sodium, on the other hand, both β_6 and β_7 are noticeably larger than L', and the cross section is closer to the expectations for a highly retarded pure $-C_7/s^7$ potential.

TABLE II. Lengths (in a.u.) which follow from the potential strength parameters $C_3=1.9009$ a.u., $C_4=5163$ a.u. for He($2\,^3S$) [31] and $C_3=1.889$, $C_4=1417$ for Na [32] according to (7) and (10) and characterize the nonretarded and retarded parts of the potential between an atom and a flat conducting surface $[\beta_3,\beta_4]$ or a conducting sphere with radius R $[\beta_6(R),\beta_7(R)]$. L and L' are R-independent lengths, (2), (6), (8), and (12), which are characteristic of the transition zone between the nonretarded van der Waals regime of comparatively small distances and the highly retarded regime at large distances.

Length	β_3	β_4	L	$\beta_6(200)$	$\beta_7(200)$	$\beta_6(2000)$	$\beta_7(2000)$	L'
He($2\,^3S$)	27740	8680	2716	1277	1560	7184	6211	3470
Na	158300	10900	750	1974	1708	11100	6803	959

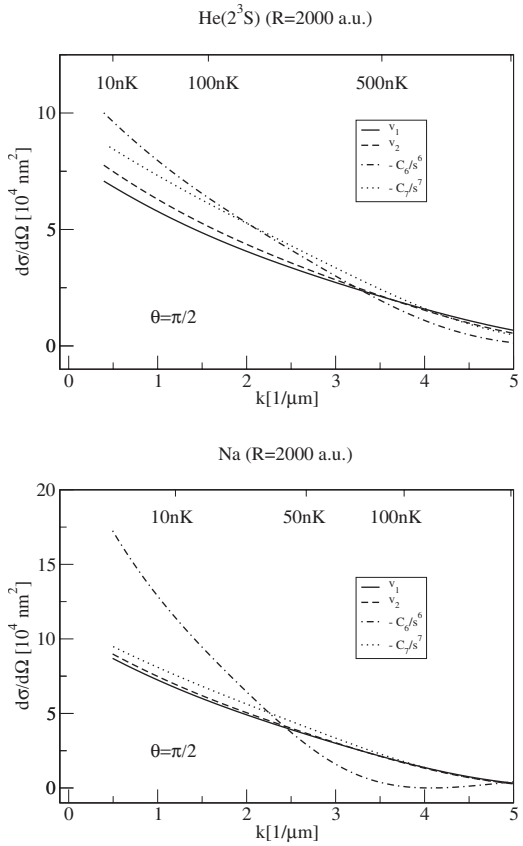

FIG. 2. Same as Fig. 1, but for $R=2000$ a.u.

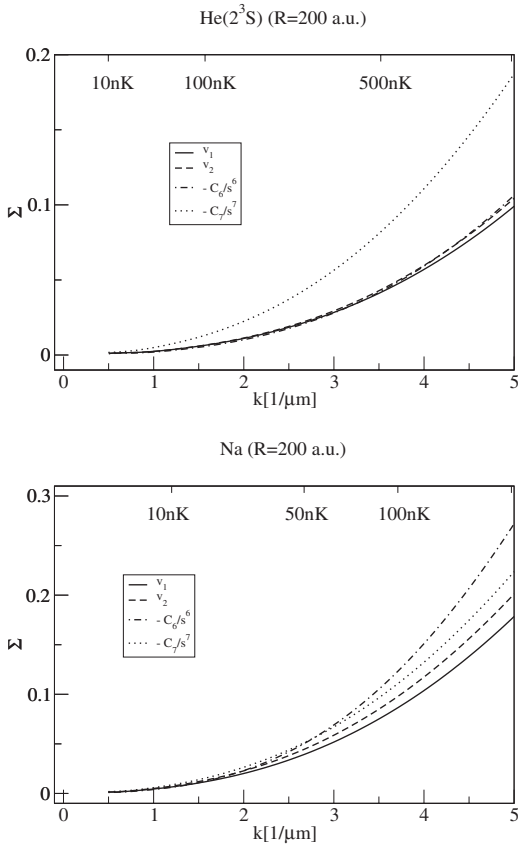

FIG. 3. Asymmetry (22) for the elastic scattering of He($2\,S^3$) atoms (top panel) and ground-state sodium atoms (bottom panel) by an absorbing sphere of radius $R=200$ a.u. The parameters C_α, β_α describing the potential strength in the nonretarded van der Waals and the highly retarded Casimir limits are as given in Table II [see also (7) and (21)]. The dotted-dashed lines show the results for a homogeneous potential $-C_6/s^6$, corresponding to a nonretarded van der Waals potential, and the dotted lines show the results for a homogeneous potential $-C_7/s^7$, corresponding to a highly retarded Casimir potential. The solid and dashed lines show the asymmetries obtained with the realistic atom-sphere potential (9) and (11) containing the two versions (13) for the shape factor describing the transition from the nonretarded to the highly retarded regime

Such an interpretation is supported by a comparison of differential cross sections (again at $\theta=\frac{\pi}{2}$) for the same atoms in the same momentum range scattered by a conducting sphere of radius 2000 a.u. as shown in Fig. 2. For sodium, both β_6 and β_7 are now much larger than L', the cross section is even closer to the expectations for a highly retarded pure $-C_7/s^7$ potential and essentially independent of the nonretarded part of the potential and its shape in the transition zone.

For helium and $R=2000$ a.u., both β_6 and β_7 are larger than L', roughly by a factor of 2, similar to the case for sodium at $R=200$ a.u. The cross sections up to $k=1/\mu$m are also similar to the results for sodium and $R=200$ a.u. in the range up to $k=5/\mu$m, which roughly corresponds to the same ranges in $k\beta_6$ or $k\beta_7$. As for sodium and $R=200$ a.u., the slope of the cross sections near threshold is quite close to the expectation for a highly retarded $-C_7/s^7$ potential, but the limiting values at threshold are not as close. The helium example shows, that increasing the radius of the sphere from 200 a.u. to 2000 a.u. raises the important characteristic lengths β_6 and β_7 to values in the distant part of the transition zone or beyond, so making the cross section less sensitive to the nonretarded and more sensitive to the highly retarded part of the atom-sphere potential.

The leading deviation from isotropy is determined by the second term in the square brackets on the right-hand side of (20), which can be studied by looking at the dimensionless asymmetry,

$$\Sigma(k) \overset{\text{def}}{=} \frac{\frac{d\sigma}{d\Omega}(\theta=0)-\frac{d\sigma}{d\Omega}(\theta=\pi)}{\frac{d\sigma}{d\Omega}(\theta=0)+\frac{d\sigma}{d\Omega}(\theta=\pi)} = 2k^2\tilde{F}(l=0,l=1)+(\text{higher-order terms}). \quad (22)$$

Figure 3 shows the asymmetry (22) for He($2\,^3S$) and Na atoms scattered by an absorbing sphere with radius 200 a.u. in the same momentum range as Figs. 1 and 2. The results for helium (top panel) are very close to the expectation for a nonretarded $-C_6/s^6$ potential (dotted-dashed line) and essentially unaffected by the potential in the transition zone and beyond. Even for sodium (bottom panel), the asymmetry is closer to the expectations for a nonretarded $-C_6/s^6$ potential than to the highly retarded $-C_7/s^7$ potential (dotted line) in

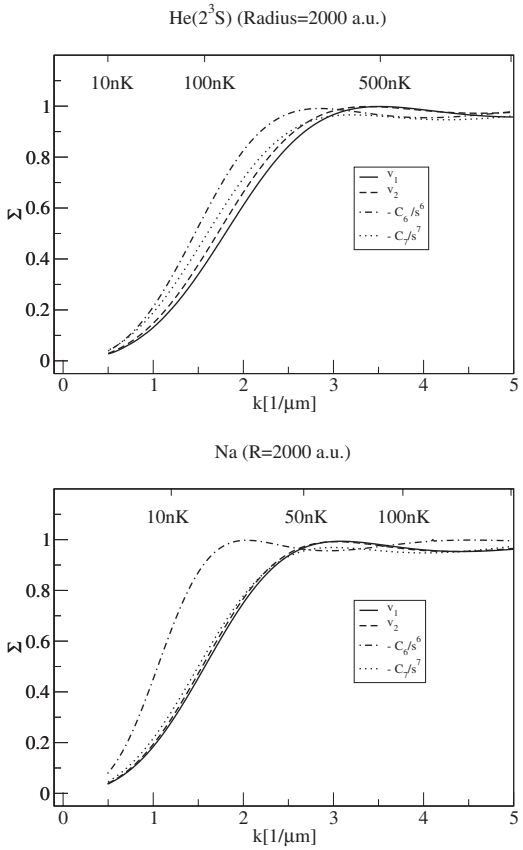

FIG. 4. Same as Fig. 3, but for $R=2000$ a.u.

the near-threshold region up to $k \approx 2/\mu$m. The asymmetries obtained with the larger radius $R=2000$ a.u. are shown in Fig. 4. The results for sodium are now very close to the expectation for a homogeneous $-C_7/s^7$ potential, even at "higher" momenta beyond the range where the near-threshold terms (20) determine the cross section. For helium and $R=2000$ a.u., the asymmetry is reproduced neither by the pure $-C_6/s^6$ potential, nor by the $-C_7/s^7$ potential, although the latter seems a better approximation for moderate wave numbers near $k=2/\mu$m. It is interesting to note, that the parameter $\tilde{F}$ in (22) vanishes for a homogeneous $-C_6/s^6$ potential with finite C_6 and $R \to 0$ [29]. This explains why the asymmetry is so much lower for the $-C_6/s^6$ potential than for the $-C_7/s^7$ potential in the top panel of Fig. 3.

V. SUMMARY

We have calculated differential cross sections for the elastic scattering of ultracold atoms by a sphere with radius in the nanometer range. Loss of flux due to inelastic reactions and adsorption is described in an unambiguous and model-independent way by imposing incoming boundary conditions in the semiclassical region near the surface of the sphere. Parameters were chosen to correspond to metastable helium ($2\,^3S$) atoms and ground-state sodium atoms scattered by a sphere with radius $R=200$ a.u. or $R=2000$ a.u. Two different shape functions (13) were used to describe the shape of the atom-sphere potential in the transition zone between the nonretarded van der Waals regime of comparatively small atom-surface separations and the highly retarded Casimir regime at large distances.

The leading near-threshold behavior of the differential cross sections is governed by a small number of tail parameters characteristic of the attractive atom-sphere potential beyond the semiclassic region at small distances. The key to understanding the results presented in Sec. IV is an appreciation of the magnitudes of the characteristic lengths β_6 and β_7 associated with the parameters C_6, C_7 defining the strength of the atom-sphere potential in the nonretarded van der Waals regime and the highly retarded regime, respectively. These characteristic lengths depend on the lengths β_3 and β_4 of the flat-surface case and on the radius R of the sphere via the very simple relation (21). By varying R, they can be tuned to lie in the nonretarded van der Waals regime, in the highly retarded Casimir regime, or in the transition zone in between. Scattering of ultracold atoms by nanospheres thus offers a transparent, sensitive and flexible possibility for probing atom-surface interactions.

ACKNOWLEDGMENT

This work was supported by the Deutsche Forschungsgemeinschaft (Grant No. FR 591/13-1)

[1] C. Henkel, J. Schmiedmayer, and C. Westbrook (Eds.), Eur. Phys. J. D **35**(1), (2005), Special Issue—Atom chips: manipulating atoms and molecules with microfabricated structures.
[2] H. B. G. Casimir and D. Polder, Phys. Rev. **73**, 360 (1948).
[3] G. Barton, J. Phys. B **7**, 2134 (1974).
[4] S. Haroche, Les Houches LIII, Course 13, 1990, p. 767.
[5] C. Carraro and M. W. Cole, Prog. Surf. Sci. **57**, 61 (1998).
[6] B. Segev, R. Côté, and M. G. Raizen, Phys. Rev. A **56**, R3350 (1997).
[7] H. Friedrich, G. Jacoby, and C. G. Meister, Phys. Rev. A **65**, 032902 (2002).
[8] F. Shimizu, Phys. Rev. Lett. **86**, 987 (2001).
[9] F. Shimizu and J. I. Fujita, Phys. Rev. Lett. **88**, 123201 (2002).
[10] V. Druzhinina and M. DeKieviet, Phys. Rev. Lett. **91**, 193202 (2003).
[11] T. A. Pasquini, Y. Shin, C. Sanner, M. Saba, A. Schirotzek, D. E. Pritchard, and W. Ketterle, Phys. Rev. Lett. **93**, 223201 (2004).
[12] H. Oberst, D. Kouznetsov, K. Shimizu, J. I. Fujita, and F. Shimizu, Phys. Rev. Lett. **94**, 013203 (2005).
[13] H. Oberst, Y. Tashiro, K. Shimizu, and F. Shimizu, Phys. Rev. A **71**, 052901 (2005).
[14] T. A. Pasquini, M. Saba, G. Jo, Y. Shin, W. Ketterle, D. E. Pritchard, T. A. Savas, and N. Mulders, Phys. Rev. Lett. **97**, 093201 (2006).
[15] A. Mody, M. Haggerty, J. M. Doyle, and E. J. Heller, Phys.

Rev. B **64**, 085418 (2001).
[16] X. W. Halliwell, H. Friedrich, S. T. Gibson, and K. G. H. Baldwin, Opt. Commun. **224**, 89 (2003).
[17] D. Kouznetsov and H. Oberst, Phys. Rev. A **72**, 013617 (2005).
[18] A. Y. Voronin, P. Froelich, and B. Zygelman, Phys. Rev. A **72**, 062903 (2005).
[19] S. Kallusch, B. Segev, and R. Côté, Eur. Phys. J. D **35**, 3 (2005).
[20] D. Kouznetsov, H. Oberst, A. Neumann, Y. Kuznetsova, K. Shimizu, J.-F. Bisson, K. Ueda, and S. R. J. Brueck, J. Phys. B **39**, 1605 (2006).
[21] A. Derevianko, J. F. Babb, and A. Dalgarno, Phys. Rev. A **63**, 052704 (2001).
[22] G. Feinberg and J. Sucher, J. Chem. Phys. **48**, 3333 (1967).
[23] B. Holstein, Am. J. Phys. **69**, 441 (2001).
[24] P. G. Burke, *Potential Scattering in Atomic Physics* (Plenum, New York, 1977).
[25] J. G. Muga, J. P. Palao, B. Navarro, and I. L. Egusquiza, Phys. Rep. **395**, 357 (2004).
[26] H. Friedrich and J. Trost, Phys. Rep. **397**, 359 (2004).
[27] F. Arnecke, H. Friedrich, and J. Madroñero, Phys. Rev. A **74**, 062702 (2006).
[28] M. J. Moritz, C. Eltschka, and H. Friedrich, Phys. Rev. A **63**, 042102 (2001).
[29] F. Arnecke and J. Madroñero (unpublished).
[30] K. G. H. Baldwin, Contemp. Phys. **46**, 105 (2005).
[31] Z.-C. Yan and J. F. Babb, Phys. Rev. A **58**, 1247 (1998).
[32] P. Kharchenko, J. F. Babb, and A. Dalgarno, Phys. Rev. A **55**, 3566 (1997).
[33] A. Derevianko, W. R. Johnson, and S. Fritzsche, Phys. Rev. A **57**, 2629 (1998).
[34] W. R. Johnson, V. A. Dzuba, U. I. Safronova, and M. S. Safronova, Phys. Rev. A **69**, 022508 (2004).